Backflashover Analysis for 110-kV Lines at Multi-Circuit Overhead Line Towers

M. Kizilcay, C. Neumann

Abstract-- An increase of back-flashovers in a 110-kV system has been observed along an overhead line route that consists of multi-circuit transmission towers of voltage levels 380-kV, 220-kV and 110-kV at the same tower. The height of multi-circuit towers varies in the range of 55 m – 88 m. The 110-kV double-circuit line is positioned at the lowest cross-arm of the tower. Influence of the various factors on the back-flashover of the 110-kV insulator strings has been studied by means of EMTP-ATP simulations. Different current waveforms of the lightning stroke have been used to represent the first stroke and subsequent strokes. Available flashover analysis methods like leader development method by Pigini et al and by Motoyama, as well as the voltage-time integration method by Kind have been implemented using a simulation language and the performance of flashover models has been compared.

The purpose of this study was to identify those towers at which back-flashover is more likely to occur than at other towers along the line route. Replacement of one insulator string of a 110-kV duplex insulator by a surge arrester is shown to be a successful mitigation technique to reduce the back-flashover rate of those 110-kV lines.

Keywords: flashover, back-flashover, lightning stroke, lightning surge, transmission tower, EMTP.

I. Introduction

The tripping of a 110-kV double-circuit overhead line has been increased in a certain region at thunder-storms, where relatively tall multi-circuit transmission towers were installed. The multi-circuit transmission route consists of 380-kV, 220-kV and 110-kV overhead lines at the same tower. Lightning strokes registered by lightning flash counters in this region showed a maximum stroke current of 90 kA. The high-frequency measurement of the tower footing resistance with a 26-kHz measuring current has revealed that the resistance value is relatively high at the three towers.

A back-flashover analysis should indicate which towers of that 5.2-km line route are rather prone to back-flashovers of the 110-kV insulation strings depending on different factors like tower footing resistance, tower surge impedance, tower height, etc. There are various methods published before to model lines, towers, lightning strokes and flashover mechanism over the insulators. Since measurements on real towers [1] are costly, various simulation models should be compared with each other to validate the simulation results.

A measure to prevent back-flashovers is to replace one insulator string of a duplex line insulator by a surge arrester. The protective level of the surge arrester for lightning strokes should be selected such that the surge arrester discharges earlier than the flashover of the insulator. Furthermore, it is important to equip a series of towers with surge arresters without leaving out a tower in-between.

The transients program EMTP-ATP with the integrated simulation language MODELS is well suited to analyze lightning surge phenomenon on overhead lines as reported several times in publications [3], [4].

II. Modeling Method

The modelling methods for the back-flashover analysis applied in this paper are based upon various publications in this field [3], [6] – [9].

A. Multi-Circuit Towers

The height of multi-circuit towers varies in the range of 55-88 m. The tower structure also varies from tower to tower along the 5.2-km route. The layout of a typical suspension tower is shown in Fig. 1. The distances are given in meters. The upper two cross-arms carry at left and right side a 220-kV and 380-kV single-circuit line, respectively. A 110-kV double-circuit line is suspended from the lowest cross-arms.

The tower is represented by loss-less *Constant-Parameter Distributed Line* (*CPDL*) model [2]. The propagation velocity of a traveling wave along a tower is taken to be equal to the light velocity, [3], [8]. The tower traveling time is $\tau_t = \frac{h}{c}$. h is the tower height.

There are several formulas to calculate the surge impedance of the tower [3], [8-10]. As a basis, the formula given in [10] for "waisted tower shape" (Fig. 2) and recommended by IEEE and CIGRE [8] is used:

$$Z_{t-waist} = 60 \cdot \ln\left[\cot\left\{0.5 \cdot \tan^{-1}\left(\frac{R}{h}\right)\right\}\right] \quad (1)$$

where $R = \frac{r_1 h_2 + r_2 h + r_3 h_1}{h}$ and $h = h_1 + h_2$.

Mustafa Kizilcay is with the University of Siegen, Department of Electrical and Computer Engineering, Siegen, Germany (e-mail: kizilcay@ieee.org).
Claus Neumann is with the RWE Transportnetz Strom, electric power utility, Dortmund, Germany (e-mail: claus.neumann@rwe.com).

Presented at the International Conference on Power Systems Transients (IPST'07) in Lyon, France on June 4-7, 2007

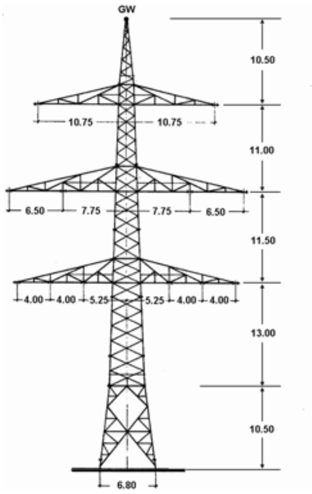

Fig. 1. Layout of a typical multi-circuit suspension tower

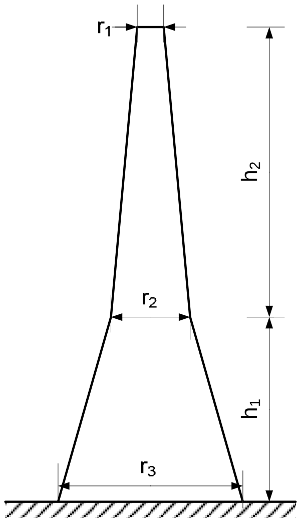

Fig. 2. "Waisted" tower shape to calculate tower surge impedance

For a tower of 76.5-m height (1) delivers the following value: $Z_{t-waist} = 233.3\,\Omega$.

It is recommended in Japan [3] to consider frequency-dependent effects for wave propagation along towers, when the tower footing impedance is represented by a linear resistance, which is the case in this study. The tower model consisting of *CPDL* model sections is added by *RL* parallel circuits at each section to represent traveling wave attenuation and distortion as shown in Fig. 3.

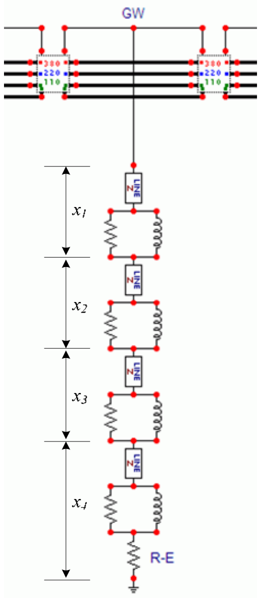

Fig. 3. Tower model with additional RL-circuits

The *RL* values are determined as functions of surge impedance Z_t, traveling time τ_t, distances between cross-arms x_1, x_2, x_3, x_4, and attenuation factor, $\alpha = 0.89$ as recommended in [3] by following equations:

$$R_i = \frac{x_i}{h} \cdot 2Z_t \cdot \ln\left(\frac{1}{\alpha}\right) \qquad (2)$$

$$L_i = 2\tau_t \cdot R_i \qquad (3)$$

The cross-arms are not represented in the tower model.

B. Number of Towers

Total 19 towers of a part of a line route shown in Fig. 4 are represented including all overhead lines. Direct lightning strokes to towers between tower #1 and #12 are analyzed.

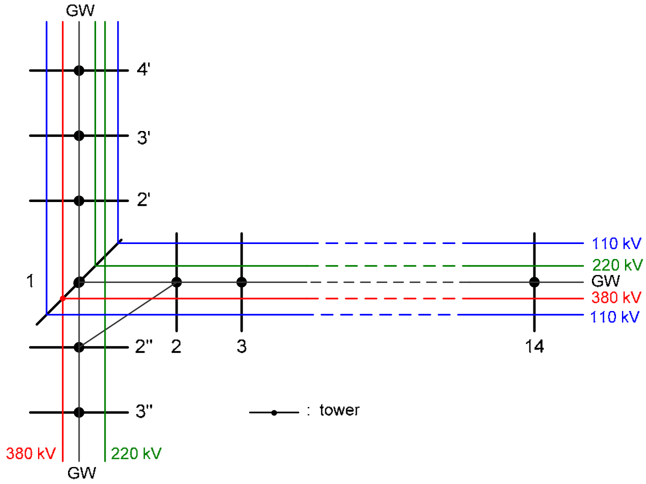

Fig. 4. Modelled part of the transmission line route with a junction at tower #1 (GW: ground wire)

C. Transmission Lines

All overhead lines at the same tower are represented by the *CPDL* model at $f = 400$ kHz. Ground wire is represented like a phase wire, which is connected to the top of the towers (see Fig. 1). Data of the conductors are:

- *380 kV*: 4 conductors/phase, ACSR 265/35 Al/St
- *220 kV*: 4 conductors/phase, ACSR 265/35 Al/St
- *110 kV*: 1 conductor/phase, ACSR 265/35 Al/St
- *ground wire*: AY/AW 216/33 (aerial cable)

In order to take into account the effect of the AC steady-state voltage of the lines on a lightning surge, the transmission lines are connected to AC voltage sources via multiphase matching impedance (surge impedance matrix).

D. Lightning Current and Impedance

The lightning stroke is modeled by a current source and a parallel resistance, which represents the lightning-path impedance. Lightning-path impedance is selected as 400 Ω according to [3].

Two different lightning current waveforms are used to represent a) first stroke and b) the subsequent strokes:

a) CIGRE waveform of concave shape with front time, $T_f = 3\ \mu s$ and time to half value, $T_h = 77.5\ \mu s$.

b) Linear ramp waveform with $T_f = 1\ \mu s$ and $T_h = 30.2\ \mu s$

In fact, according to [8] the front time of the first stroke depends on the peak value of the lightning current. In this study T_f and T_h are assumed to be constant. The maximum rate-of-rise S_m of the current has been so adjusted, that the ratio I/T_f to S_m corresponds to the average values of a first stroke: $I = 31$ kA, $S_m = 26$ kA/μs, $T_f = 3$ μs [8]. Fig. 5 shows both current waveforms with a magnitude of 50 kA.

E. Flashover Models

Flashover models estimate the breakdown of the air between the arcing horns of the line insulators under non-standard wave forms.

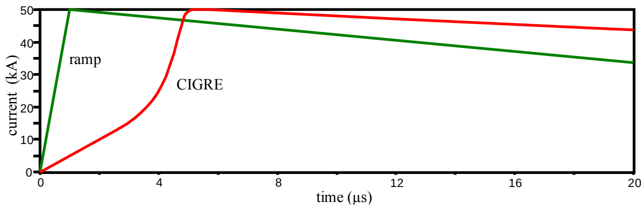

Fig. 5. Lightning current waveforms; CIGRE concave waveform, linear ramp function

In the literature there are mainly two methods are known besides the simple flashover estimation by means of a volt-time curve of an insulator [7], [8]. They are integration methods and Leader development methods. In this study three flashover models are applied for comparison purposes.

a) Equal-area criterion by Kind [6], [8], [14];
b) Leader development method by Motoyama [4], [12];
c) Leader development method by Pigini et al. [8], [13].

Wave deformation due to corona is not considered in the lightning surge simulations. The surge propagating on the ground wire can be normally deformed by corona. In this paper it is assumed that the lightning stroke terminates at the tower.

1) Equal-area criterion by Kind

The criterion by Kind requires two parameters, U_0 and F, and it is tested simply by evaluating the following integral numerically:

$$\int_0^{t_{flo}} \left[u(t) - U_0\right] dt \geq F \quad (4)$$

where *u(t)* is the voltage waveform across the insulator.

When the time integral of the voltage difference ($u - U_0$) becomes greater than the value of F, then at $t = t_{flo}$ the flashover occurs. In other words, any impulse voltage waveform can lead to a flashover, if a certain volt-time area will be covered. The unknown parameters U_0 and F can be obtained from the 50 % sparkover volt-time characteristic of the insulator [16]. This characteristic is established as a function of the insulator length [7] and alternatively, from the known arcing distance of the 110-kV insulators [15]. Both curves are very close to each other and shown in Fig. 6. The unknown parameters in (5) are determined according to [16]: $U_0 = 475.42$ kV, $F = 0.304$ Vs.

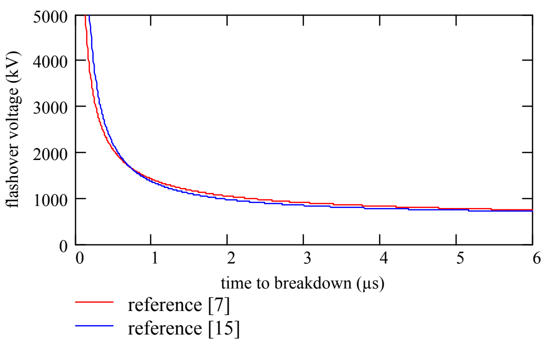

Fig. 6. 50 % flashover volt-time curve of the 110-kV insulator

2) Leader development method by Motoyama

Leader development methods for flashover analysis gives special consideration to physical aspects associated with the discharge mechanism [7], [8]. The flashover model by Motoyama [12] is developed for short tail lightning impulse voltages. It is based on experiments for 1m…3m gap lengths. The leader onset condition for positive polarity is used:

$$\frac{1}{T_s}\int_0^{T_s} u(t)dt = U_{ave} \; > \; 400(kV)\cdot D(m) + 50(kV) \quad (5)$$

where *u(t)* is the imposed voltage between archorns and *D* is the gap length in meter. T_s is the streamer developing time (= leader onset time). The leader developing process is defined by following equations:

$$v_{LAVE} = \begin{cases} K_{1A}\cdot\left(\dfrac{u(t)}{D-2x_{LAVE}(t)} - E_0\right) & \text{for } 0 \leq x_{LAVE} < D/4 \\ K_{1B}\cdot\left(\dfrac{u(t)}{D-2x_{LAVE}(t)} - E_0\right) & \text{for } D/4 \leq x_{LAVE} < D/2 \end{cases} \quad \text{(m/s)} \; (6)$$

$$x_{LAVE}(t) = \int v_{AVE}(t)\,dt \quad \text{(m)} \quad (7)$$

$$q_L = 2K_0 \cdot x_{LAVE} \quad \text{(C)} \quad (8)$$

where q_L is the charge accumulated in the leader; x_{LAVE} is the average value of the leader-developing length; and v_{LAVE} is the leader-developing velocity. The constants E_0, K_0, K_{1A}, K_{1B} are set to 750 kV/m, 410 µC/m, 2.5 m²/(Vs) and 0.42 m²/(Vs), respectively.

The breakdown occurs when x_{LAVE} attains *D/2*. If the applied voltage *u(t)* becomes less than $E_0\cdot(D-2x_{LAVE})$ during a leader-developing process, the leader is considered to stop its development.

3) Leader development method by Pigini et al.

The flashover condition is estimated by the imposed voltage across the air gap. The leader onset condition is given as [13]

$$u(t) \geq E_{0p}\cdot D \quad (9)$$

where D is the gap length and $E_{0p} = 670$ kV/m.

The equivalent leader-developing velocity v_l (m/s) is computed according to following equation, which was evaluated by several measurements [13]:

$$v_l = 170\cdot D\cdot\left(\frac{u(t)}{D-l_l} - E_{0p}\right)\cdot\exp\left(0.0015\cdot u(t)/D\right) \quad (10)$$

where l_l is the leader length in meter; *u(t)* is the voltage imposed to the air gap. The leader length is obtained by the integral of leader-developing velocity:

$$l_l = \int v_l(t)\,dt \quad (11)$$

The breakdown occurs, when the leader length l_l is equal to the gap length D.

4) Representation of the Air Gap Breakdown

The discharge in the air gap can be represented by a time-dependent arc resistance, decreasing from 1 kΩ, to 1Ω in 0.1 µs and to 0.1Ω in 1 s, based on [14].

III. Back-Flashover Performance Estimation

In order to estimate roughly which towers on the route from tower #1 to #12 (Fig. 4) are endangered by back-flashovers across 110-kV insulators, a systematic analysis is performed. Following two lightning current waveforms are injected to each tower in question.

– CIGRE waveform, $I = 20 \cdots 90$ kA; $3\ \mu s / 77.5\ \mu s$

– Linear ramp function, $I = 20 \cdots 90$ kA; $1\ \mu s / 30.2\ \mu s$.

The current amplitude has been increased in 5 kA steps from 20 kA up to 90 kA and back-flashover across the 110-kV insulators has been examined simultaneously by the three flashover models. The simulation results are summarized in figures 7 and 8 for the two current waveforms. In those diagrams the minimum lightning peak current is shown that causes a back-flashover at the 110-kV insulator. Following observations are made regarding back-flashovers:

– Generally towers #3, #4, #5, #8, #9 are more likely to produce a back-flashover than the other towers.

– The back-flashover at the towers depends on the current waveform as expected.

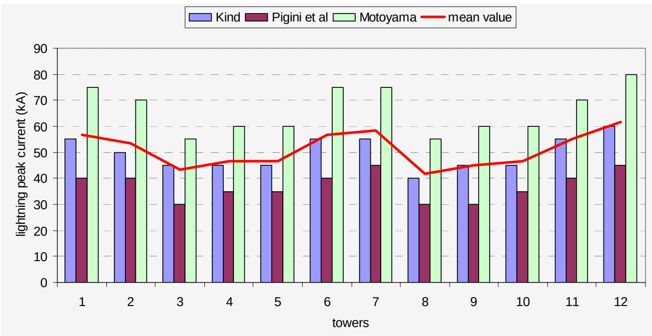

Fig. 7. Minimum lightning peak currents of CIGRE waveform (3/77.5 µs) causing back-flashover at the 110-kV insulators

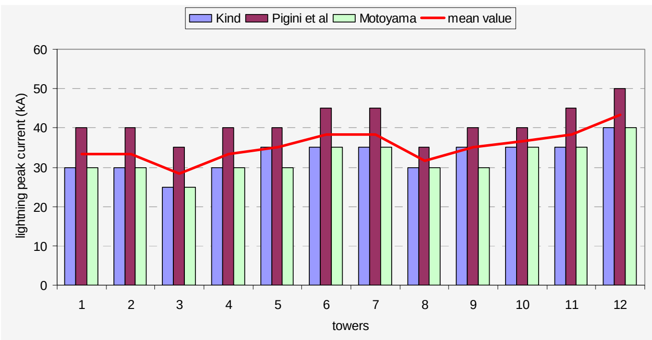

Fig. 8. Minimum lightning peak currents of linear ramp type (1/30.2 µs) causing back-flashover at the 110-kV insulators

– The flashover models perform differently depending on the lightning current waveform. The flashover model by Motoyama produces conservative results in Fig. 8 compared to the other two models, i.e. the flashovers occur at higher lightning currents. A similar behavior can observed by the method of Pigini in the case of steep linear ramp function. The equal-area criterion by Kind performs well in both cases.

– There is a clear inverse correlation between the flashover tendency and the tower footing resistance, and a rather weak correlation between the flashover tendency and tower surge impedance can be observed in Fig. 9.

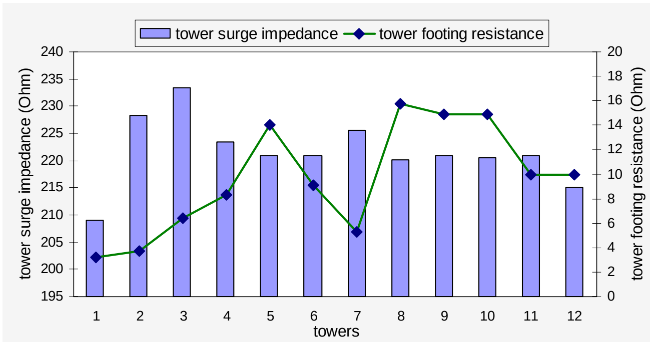

Fig. 9. Tower surge impedances and measured footing resistances

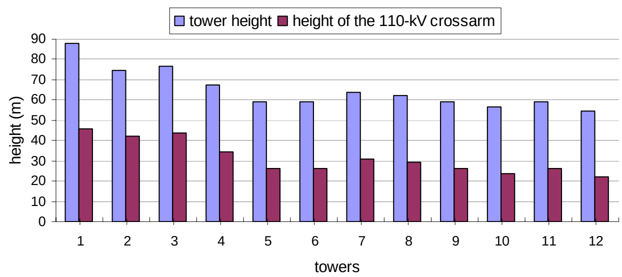

Fig. 10. Height of towers and crossarms of the 110-kV line

Another factor influencing the flashover performance of the 110-kV insulators is the height of the tower and crossarm of the 110-kV line as shown in Fig. 10.

Taking the probability distribution relation for lightning crest current magnitudes according to IEEE [9]

$$p(i > I) = \frac{1}{1 + \left(\dfrac{I}{31\ \text{kA}} \right)^{2.6}} \qquad (12)$$

into consideration, it can be said that at the mostly endangered towers #3 and #8 with an average peak value of $I = 36$ kA, 40 % of lightning strokes would cause a back-flashover across 110-kV insulators.

IV. Mitigation Of Back-Flashovers By Line Surge Arresters

Line surge arresters parallel to the phase insulators of 110 kV circuits prevent back-flashovers at those towers [18].

Towers #3, #5 and #8 are selected as endangered towers by back-flashovers of the 110-kV lines and are equipped with line surge arresters, which replace one insulator string of the duplex insulator of the double-circuit 110-kV line. The model referring to [17] of the selected surge arrester with rated voltage of 156 kV and its nonlinear voltage-current characteristic are shown in figures 11 and 12, respectively.

It can be easily checked by the Kind equal-area criterion that no flashover can occur across the insulator string parallel to the surge arrester, because the voltage across the insulator will be limited by surge arresters below U_0 in (4).

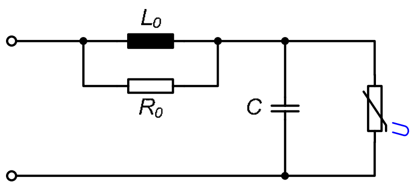

$L_0 = 0.307\ \mu H$; $R_0 = 153.5\ \Omega$; $C = 65.1$ pF

Fig. 11. Surge arrester model

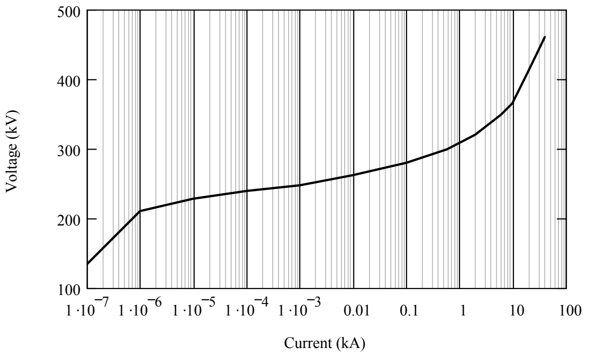

Fig. 12. Voltage-current characteristic of the surge arrester

The simulations of lightning strokes with $I = 200\ \text{kA}; 3\ \mu s / 77.5\ \mu s$ at the towers #3 and #8 confirmed also that no breakdown can occur across parallel insulators according to the other two flashover models by Pigini et al and Motoyama. Due to discharging of the surge arresters (see Fig. 13) the voltage of the 110-kV phase conductors temporarily increases significantly. Fig. 14 shows voltages of phase *c* at the towers #1, #2, #3, #4 and #5, when a lightning stroke with $I = 100\ \text{kA}; 3\ \mu s / 77.5\ \mu s$ hits the top of the tower #3. The operating 50-Hz voltage of phase *c* is at moment of the lightning stroke equal to the negative peak value (–90 kV). Depending on the amplitude of the discharge current of surge arresters, a flashover may take place at other towers, which are not equipped with surge arresters. In this respect two cases have been studied: lightning stroke to towers #3 and #8, which are equipped with line surge arresters for 110 kV. Adjacent towers do not contain any line surge arresters.

The CIGRE current waveform with 3/77.5 μs as lightning stroke is used by increasing the amplitude in 5 kA steps. The flashover condition is checked by the Kind equal-area criterion. At tower #3, when $I > 95$ kA and at tower #8, when $I > 90$ kA, a flashover is expected at the adjacent towers across the 110-kV phase insulators.

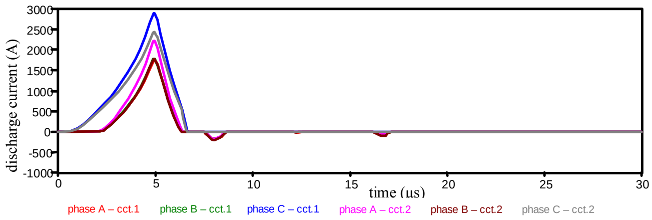

Fig. 13. Discharge current of the six line surge arresters at tower #3 (no flashover at adjacent towers is assumed)

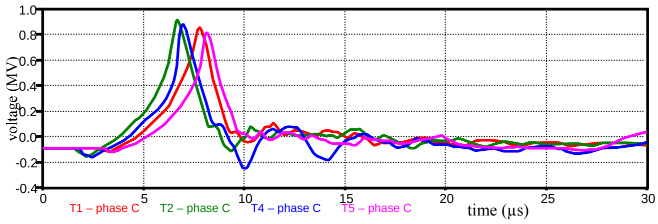

Fig. 14. Voltages between phase c and the tower at towers #1, #2, #4 and #5 of the 110-kV line due to discharging of line surge arresters at tower #3. No flashover at adjacent towers is assumed.

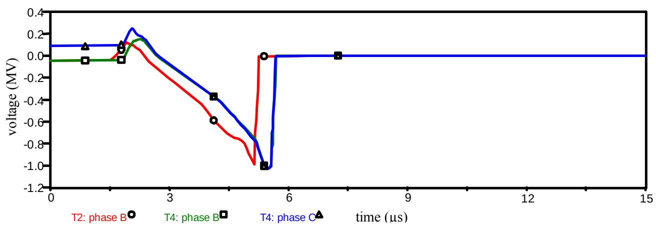

Fig. 15. Waveforms of voltages across 110-kV phase insulators with flashovers at towers #2 and #4 (no line surge arresters are installed at those towers)

Waveforms of the voltage across flashed-over insulators are shown in Fig. 15 for the case of lightning stroke to tower #3 with 110 kA. At tower #2 the phase *b* and at tower #4 the phases *b* and *c* attain flashover.

An important question is, how well the surge arresters will perform in terms of energy absorption. A lightning stroke with $I = 200\ \text{kA}; 3\ \mu s / 77.5\ \mu s$ is applied as worst-case to the top of towers #3 and #8. It is assumed that no line arresters are installed at adjacent towers. Consequently, flashover takes place in all phases of the 110-kV double-circuit line at adjacent towers. Maximum energy absorption computed is 34 kJ, which is uncritical.

V. Conclusion

A systematic flashover analysis has been performed for a 110-kV double-circuit overhead line, which is a part of a multi-circuit transmission route. Two different lightning stroke current waveforms have been applied. The back-flashover performance is estimated by means of three different flashover models. The towers at which back-flashover is more likely than at others are identified in order to take countermeasures like replacement of one 110-kV insulation string by a surge arrester at those towers.

Multi-circuit tower system is modeled with the graphical preprocessor ATPDraw and the simulations are performed using EMTP-ATP. It has been shown that line surge arresters can be successfully utilized to prevent back-flashovers across 110-kV phase insulators at endangered towers. For lightning stroke current amplitudes greater than 90 kA, flashover may occur at the adjacent towers due to discharge current of operated surge arresters, when the phase conductors at those towers are not equipped with surge arresters. Energy absorption of the selected 110-kV line arresters remains uncritical.

VI. References

[1] Yamada, T.; Mochizuki, A.; Sawada, J.; Zaima, E.; Kawamura, T.; Ametani, A.; Ishii, M.; Kato, S.: "Experimental Evaluation of a UHV Tower Model for Lightning Surge Analysis", IEEE Trans. on Power Delivery, Vol. 10, No. 1, pp. 393-402, Jan 1995.

[2] Canadian/American EMTP User Group: *ATP Rule Book*, distributed by the European EMTP-ATP Users Group Association, 2005.

[3] Ametani, A.; Kawamura, T.: "A Method of a Lightning Surge Analysis Recommended in Japan Using EMTP", IEEE Trans. on Power Delivery, Vol. 20, No. 2, pp. 867-875, April 2005.

[4] Mozumi, T.; Baba, Y.; Ishii, M.; Nagaoka, N.; Ametani, A.: "Numerical Electromagnetic Field Analysis of Archorn Voltages During a Back-Flashover on a 500-kV Twin-Circuit Line", IEEE Trans. on Power Delivery, Vol. 18, No. 1, pp. 207-213, Jan. 2003.

[5] Dommel, H. W.: *EMTP Theory Book*, Bonneville Power Administration, conversion into electronic format by Can/Am EMTP User Group in 1995.

[6] Schmitt, H.; Winter, W.: "Simulation of Lightning Overvoltages in Electrical Power Systems", Proceedings IPST 2001 (International Conference on Power System Transients), Rio de Janerio, June 24-28, 2001.

[7] IEEE Fast Front Transients Task Force, Modeling and Analysis of System Transients Working Group: "Modeling Guidelines for Fast Front Transients", IEEE Trans. on Power Delivery, Vol. 11, No. 1, pp. 493-506, Jan. 1996.

[8] CIGRE WG 33-01: "Guide to Procedures for Estimating the Lightning Performance of Transmission Lines", Technical Brochure, October 1991.

[9] IEEE Working Group on Lightning Performance of Transmission Lines: "A Simplified Method for Estimating Lightning Performance of Transmission Lines", IEEE Trans. on Power App. & Systems, Vol. PAS-104, No. 4, pp. 919-927, April 1985.

[10] Chisholm, W. A.; Chow, Y. L.; Srivastava, K. D.: "Travel Time of Transmission Towers", IEEE Trans. on Power App. and Systems, Vol. PAS-104, No. 10, S. 2922-2928, Oktober 1985.

[11] IEEE Working Group on Estimating the Lightning Performance of Transmission Lines: "IEEE Working Group Report – Estimating Lightning Performance of Transmission Lines II – Updates to Analytical Models", IEEE Trans. on Power Delivery, Vol. 8, No. 3, pp. 1254-1267, July 1993.

[12] Motoyama, H.: "Experimental study and analysis of breakdown characteristics of long air gaps with short tail lightning impulse", IEEE Trans. on Power Delivery, Vol. 11, No. 2, pp. 972-979, April 1996.

[13] Pigini, A.; Rizzi, G.; Garbagnati, E.; Porrino, A.; Baldo, G.; Pesavento, G.: "Performance of large air gaps under lightning overvoltages: Experimental study and analysis of accuracy of predetermination methods", IEEE Trans. on Power Delivery, Vol. 4, No. 2, pp. 1379-1392, April 1989.

[14] Fernandes, M.; Correia de Barros, M. T.; Ameida, M.E.: "Statistical Study of the Lightning Overvoltages at a Gas Insulated Station Transformer", Proceedings IPST 1995 (International Conference on Power System Transients), Lisbon, 3-7 September 1995.

[15] Koettniz, H.; Winkler, G.; Weßnigk, K.-D.: Fundamentals of Electrical Operational Phenomena in Electrical Power Systems, (original title in German: Grundlagen elektrischer Betriebsvorgänge in Elektroenergie-systemen), Deutscher Verlag für Grundstoffindustrie, Leipzig, 1986.

[16] CIGRE WG 33.02: "Guidelines for representation of network elements when calculating transients", CIGRE Technical Brochure, No. 39, 1990.

[17] IEEE Working Group 3.4.11-Surge Protective Devices Committee: "Modeling of Metal Oxide Surge Arresters", IEEE Trans. on Power Delivery, Vol. 7, No. 1, pp. 302-309, Januar 1992.

[18] Tarasiewicz, E. J.; Rimmer, F.; Morched, A. S.: "Transmission Line Arrester Energy, Cost, and Risk of Failure Analysis for Partially Shielded Transmission Lines", IEEE Trans. on Power Delivery, Vol. 15, No. 3, pp. 919-924, July 2000.

VII. Biographies

Mustafa Kizilcay was born in Bursa, Turkey in 1955. He received the B.Sc. degree from Middle East Technical University of Ankara in 1979, Dipl.-Ing. degree and Ph.D. degree from University of Hanover, Germany in 1985 and 1991. From 1991 until 1994, he was as System Analyst with Lahmeyer International in Frankfurt, Germany. 1994-2004 he has been professor for Power Systems at Osnabrueck University of Applied Sciences, Germany. Since 2004 he is with the University of Siegen, Germany, holding the chair for electrical power systems as full professor. Dr. Kizilcay is winner of the literature prize of Power Engineering Society of German Electro-engineers Association (ETG-VDE) in 1994. His research fields are power system analysis, digital simulation of power system transients and dynamics, insulation-coordination and protection. He is a member of IEEE, CIGRE, VDE and VDI in Germany.

Claus Neumann studied electrical engineering at the Technical University of Aachen. After finishing with the Dipl.-Ing. degree in 1972 he was engaged as a testing engineer in the high voltage and insulating material laboratory of a switchgear manufacturer. In 1979 he joined the department for HV equipment of RWE in Essen, Germany. Among others he worked on non-standardised stresses of switchgear in the network, on testing technique, monitoring and diagnostics and on maintenance strategies. In 1992 he became head of this department. In 1992 he also received his Dr.-Ing. degree from the Technical University of Darmstadt. In 2001 he became Honourable Professor at the Technical University of Darmstadt where he gives a lecture in HV switchgear and substations. Since 2005 is in charge of the Operational Asset Management at RWE Transportnetz Strom, Dortmund, Germany. His main fields of activity are fundamental design and layout of HV apparatus and asset management including maintenance and renovation strategy, monitoring and diagnostics, environmental impact of SF6 technology etc.. He is among others a member of CIGRE Study Committee C4, Power System Performance, of CIGRE SC D1 Working Group 3, Gas-insulated Systems.